Stability and electronic properties of complex structures of silicon and carbon under pressure: Density-functional calculations

R. Biswas

Microelectronics Research Center, Iowa State University, 1925 Scholl Road, Ames, Iowa 50011

Richard M. Martin

Xerox Corporation, Palo Alto Research Center, 3333 Coyote Hill Road, Palo Alto, California 94304

R. J. Needs

Cavendish Laboratory, University of Cambridge, Madingley Road, Cambridge CB3 0HE, United Kingdom
and Xerox Corporation, Palo Alto Research Center, 3333 Coyote Hill Road, Palo Alto, California 94304

O. H. Nielsen

Nordisk-Institut for Teoretisk Atomfysik (NORDITA), Blegdamsvej 17, DK-2100 Copenhagen, Denmark

The structural and electronic properties of the complex tetrahedral structures B-8 (or "BC8," bcc with 8 atoms per cell) and T-12 (or "ST12," simple tetragonal with 12 atoms per cell) phases of sil- icon and carbon are computed with *ab initio* density-functional calculations of the energy, pressure, and enthalpy. For silicon, the B-8 and T-12 phases are found to be metastable, consistent with their formation during pressure reduction in high-pressure experiments. Energies of both structures are close to that of amorphous silicon. T-12 has an indirect gap larger than diamond-structure Si whereas B-8 is semimetallic. For carbon, the B-8 phase is found to be stable, relative to diamond and all previously calculated metallic phases, above pressures of 12 Mbar. This represents a new limit for the stability of diamond.

I. INTRODUCTION

A variety of phases for elemental silicon and germanium can be produced by the use of pressure. In particular for silicon, at a pressure of ~125 kbar the diamond-structure phase transforms to the metallic body-centered-tetragonal β-tin structure,[1,2] that has been recently observed to further transform to a novel simple hexagonal structure at pressures in the range of 140—160 kbar.[3] The atomic coordination systematically increases from 4 to approximately 6 and 8 in these pressure-induced transitions. The metallic β-tin and simple hexagonal phases have recently been found to be superconducting[4] with transition temperatures as high as 8—9 K (Ref. 4) and there is much interest in the dependence of the transition temperatures with pressures. For germanium the β-tin phase has also been observed at pressures of ~100 kbar, although the simple hexagonal phase has only been seen at much higher pressures [800 kbar (Ref. 5)].

In addition, reducing or quenching the pressure from the β-tin phases of both silicon and germanium produces complex crystal structures with large primitive cells and locally distorted tetrahedral coordination.[6—8] Two accurately characterized complex structures are B-8 (or "BC8," body-centered cubic with 8 atoms/cell) T-12 (or "ST12," simple tetragonal with 12 atoms/cell).[6,7] These complex phases remain metastable with respect to diamond at ambient pressures, and much thermal treatment is required to convert these complex structures back to the diamond form.[6,7] The local bonding geometries of B-8 and T-12 are distortions of tetrahedral with 2 or more bond lengths and a distribution of bond angles. However the distorted tetrahedra in these phases are packed in a more efficient space-filling-way than diamond resulting in densities larger than diamond, but smaller than the closer packed metallic structures. An understanding of these dense, covalent structures is essential for study of the phase diagrams of group-IV elements.

These complex structures have also been of interest from other points of view. In previous work,[8] the sequence of increasingly complex crystal structures: diamond—wurtzite—B-8—T-12, has been used to study the manner in which the properties of the amorphous structure develop from increasing short-range disorder in the crystalline phase. The optical properties of T-12, which has fivefold and sevenfold rings, were found to be similar to those for amorphous silicon.[8] The distorted tetrahedral geometries and the odd-numbered ring topologies are similar to those proposed for grain boundaries in silicon,[9,10] and for "π-bonded" reconstructions of the Si(111) surface.[11]

In the present work we also consider carbon in these complex tetrahedral phases, which we find to be more stable than diamond at large enough pressures. The stability of diamond (carbon) is of interest to many fields of science, and has been a subject of much continuing discussion,[12] though little has been established experimentally. A stability limit for diamond provides a theoretical upper

bound to the pressures that may be achieved with diamond anvil cells. To date, diamond anvil cells have attained pressures of 1.7 Mbar (Ref. 13) (and possibly higher), and the extension to higher pressures could provide crucial experimental tests, e.g., for the existence of metallic hydrogen, for which predictions of the metallization pressure range between 2 and 10 Mbar.[14] Predictions for pressure-induced transitions of a number of elemental metals and nonmetals also exist.[15]

Previous studies have estimated stability limits on diamond carbon based on simple analogies with the metallic phase of silicon (β-tin).[16] However, Yin and Cohen[17] have found diamond-carbon stable against all simple metallic phases considered up to the very high pressure of 23 Mbar, at which point the simple cubic phase was more stable. These results illustrate an essential difference between metallic silicon and carbon phases.

In this paper we investigate the relative stability of silicon and carbon in the complex tetrahedral and diamond structures (and for Si, β-tin also), with *ab initio* density-functional calculations. We describe extensive results for B-8 and limited results for other complex structures. Some of these results have been presented in a Brief Report.[18] Closely related calculations have been also presented by Yin.[19] Relative to the previously published work,[18] this paper contains new results and discussions on the bonding topology of B-8 and T-12 phases, the packing fractions of these phases and connections to surface reconstructions. In this paper new calculations for the enthalpy of Si phases are presented, further results for the electronic properties of B-8 and T-12-Si are described and a soft mode of T-12 is identified. The role of zero-point energies in altering the structural stabilities is also discussed. This paper is organized into six sections. First the B-8 and T-12 structures are described in detail in Sec. II, followed by a brief account of the density-functional method in Sec. III. Our results for silicon and carbon are presented in Secs. IV and V, respectively.

II. THE B-8 AND T-12 STRUCTURES

The structures of the B-8 and T-12 phases have been studied with very precise x-ray diffraction techniques. The structural geometries of these phases are summarized here.

A. B-8

Figure 1 is a projection of the B-8 structure on a (001) plane, with elevations of atoms in units of $a/10$, a being the cube side. The connectivity of the tetrahedra is such as to produce a body-centered cubic Bravais lattice with an 8-atom basis and a space group $Ia3$ (T_h^7).[20] All the 8 sites in the primitive cell are equivalent, i.e., they have the same local environment. The atoms in B-8 form sixfold rings though these rings are substantially distorted from those in diamond. Relative to the plane of the ring, the B-8 atoms consecutively occupy d,d,u,u,d,u positions (d: down, u: up) in comparison to alternating u, d positions in diamond. Locally, each atom is connected to four neighbors by one type-A bond and three type-B bonds,
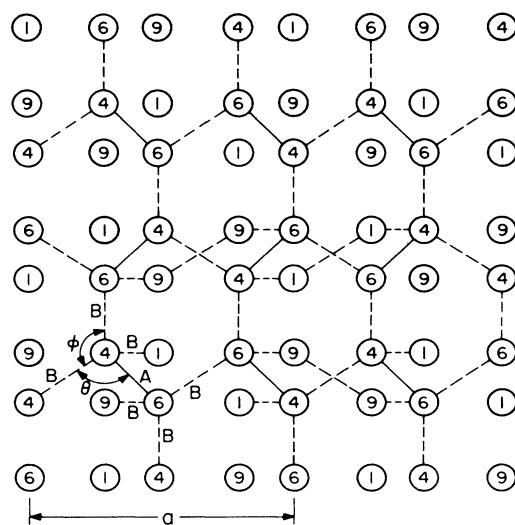
FIG. 1. Projection of the B-8 Si structure on a (001) plane. The numbers are the elevations of the atoms, above the xy plane, in units of $a/10$. a is the cubic lattice constant. All atoms are equivalent.

with the zero-pressure B-8 silicon structure experimentally found to have shorter A bonds ($R_A = 2.30$ Å) and longer B bonds ($R_B = 2.39$)Å.[6,21] These bonds form two inequivalent bond angles (AB, BB) which are $\simeq 99°$ and 117° for the zero-pressure structure. Though more dense, the average nearest-neighbor distances in B-8 (and even T-12 and β-tin) are larger than diamond, indicating weaker covalent bonding in the complex structures. The packing fraction of B-8 is $\sim 10\%$ larger than that of diamond (at the zero-pressure structure), as indicated in Table I.

The B-8 structure is completely specified by one internal parameter x and the lattice constant a. In terms of these variables the A bond length is simply

$$R_A = 2\sqrt{3}x \text{ (in units of } a) . \tag{1}$$

The B bonds have a length of

$$R_B = (0.25 - 2x + 8x^2)^{1/2} \text{ (in units of } a) . \tag{2}$$

The difference between the bond lengths is determined by the internal parameter x, with $R_A < R_B$ for $x < 0.1036$, whereas $R_A > R_B$ for $x > 0.1036$, with $x = 0.1003 \pm 0.0008$

TABLE I. Packing fractions for structures. The packing fractions for B-8 and β-tin were for the calculated minimum energy structure, and for T-12 the calculated lowest energy structure.

Structure	Packing fraction
Diamond	0.340
B-8	0.372
T-12	0.385
β-tin	0.551

for the experimental zero-pressure structure. The two bond angles, however, depend only on x and are given through

$$\cos(AB) = \frac{(8x^2 - x)}{2\sqrt{3}x(0.25 - 2x + 8x^2)^{1/2}}, \quad (3)$$

and

$$\cos(BB) = \frac{(4x^2 - x)}{(0.25 - 2x + 8x^2)}. \quad (4)$$

AB is smaller than the tetrahedral angle, whereas BB is larger, and the distortion of the angles from tetrahedral is a monotonically increasing function of x.

The B-8 structure has a center of inversion which is the midpoint of any A bond. These A bond centers lie on a simple cubic lattice. As is evident from Fig. 1, the A bonds are oriented in [111] directions, whereas the B bonds lie in $[x,y,0]$ or equivalent planes. Further, all the bonds are "staggered," i.e., the dihedral angles in this structure are 60°, similar to diamond, but unlike wurtzite.

As is evident from Fig. 1 B-8 forms double layers perpendicular to a [100] direction, with all the A bonds lying within the atomic double layers. Further, an interesting atomic surface can be formed by cleaving the B-8 crystal.

Cutting the crystal normal to a [100] direction and between two double layers breaks the least number of bonds (all B bonds) and leads to a natural cleavage plane for B-8. The resulting (100) B-8 surface has a density of $\simeq 11.02$ Å^2/surface atom, which is comparable to a density of 12.77 Å^2/surface atom for the Si (111) surface. Structurally the B-8 (100) surface consists of dimers. Atoms of the dimers have one surface B-bond, two bonds extending into the surface, and one dangling bond—this geometry being very similar to the dimers formed on a reconstructed Si(100) surface.[22] There may well be other interesting topological similarities between the distorted tetrahedral geometries of these complex structures and the reconstructions observed on semiconductor surfaces.

B. T-12

T-12 is a more complex structure than B-8 and Fig. 2 shows a projection of the T-12 structure on an (001) plane with elevations of atoms in units of $c/4$. Though not observed for Si, the T-12 structure is well documented in Ge.[7] The Bravais lattice is simple tetragonal ($a = 5.93$ Å, $c = 6.98$ Å) with 12 atoms in the primitive cell, generating the space group $P4_32_12$ (D_4^8) or its mirror image $P4_12_12$ (D_4^4).[20] The atoms in this structure occupy two inequivalent sites in the primitive cell and, are connected together to form fivefold and sevenfold rings. Because of these features, T-12 has been proposed as a model containing local arrangements similar to amorphous semiconductors.

T-12 has three different bond lengths ($A = 2.47$ Å, $B = 2.44$ Å, and $C = 2.55$ Å for Ge at zero pressure) and a spread of bond angles from 90° to 130°, so than the tetrahedra are substantially more distorted in T-12 than in B-8. T-12 has a packing fraction of ~ 0.38 similar to B-8 and larger than diamond (0.34), as indicated in Table I.
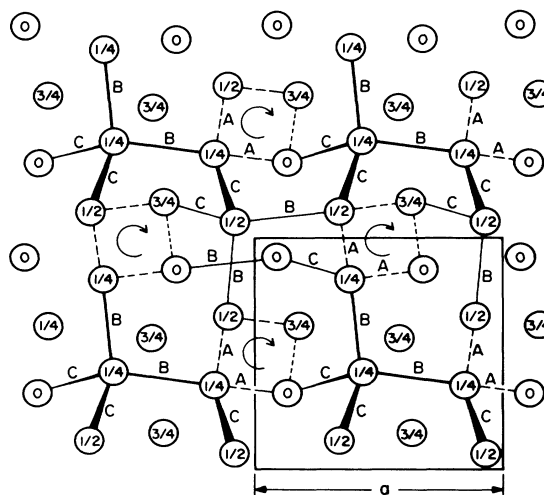
FIG. 2. Projection of the T-12 Si structure on a (001) plane, with elevations of the atoms shown in units of $c/4$. The unit cell is outlined. The A bonds (dotted lines) mark out the spirals along the (001) axis, and their direction of rotation is shown (arrows). The unit cell contains two inequivalent sites: (i) atoms having A,A,B,C bonds lying within the spirals and (ii) atoms with B,B,C,C, bonds that connect adjacent spirals.

There are four internal parameters in T-12 (α, x, y, and z) which have the measured values $\alpha = 0.1$, $x = 0.166$, $y = 0.375$, $z = 0.25$ in Ge.[6] We schematically denote the two inequivalent atoms in the unit cell as four type-I and eight type-II atoms. As indicated in Fig. 2, atoms of type II form fourfold spirals in the z direction. The spirals have pitch c and are entirely comprised of A bonds between type-II atoms. Atoms on adjoining spirals are linked together through type-I atoms with B- and C-type bonds. The choice of $z = \frac{1}{4}$ requires the elevations of atoms in the spirals to be multiples of $c/4$, as shown in Fig. 2. For other values of z, the spirals are less symmetrical although the bond angles within the spirals always remain 90°.

The symmetry operation relating the two spirals in the unit cell is a rotation of 90° around the c axis passing through the origin, followed by a translation of $(a/2, a/2, c/4)$, i.e., a screw rotation. All the T-12 spirals rotate in the same direction giving the structure optical activity or a definite helicity. Consequently T-12 lacks an inversion center, since inversion would produce the enantiomorph where the rotation of the spirals is reversed. Fivefold and sevenfold ring geometries are a way to approximately preserve local tetrahedral bonding without large lattice strains, and are a general feature of amorphous semiconductors and surface reconstructions such as the chain model for the reconstructed 2×1 Si(111) surface,[11] as well as, for models of edge dislocations and twin boundaries in silicon.[9,10]

III. DENSITY-FUNCTIONAL STUDIES

The calculations described in the following sections for silicon and carbon, employ the well-known density-functional method[23] in the reciprocal-space formalism.[24,25] We study the properties of the complex structures with the simultaneous calculations of the energy E, forces, pressure P, enthalpy $H = E + PV$, macroscopic stresses, and the self-consistent electron density. A generalization of the viral theorem, known as the stress theorem,[26] allows the components of the stress tensor to be analytically expressed in terms of the electronic charge density and the variational wave functions.[26] The additional structural information in calculations of forces and stresses were essential to relax the complex structures, i.e., the atomic positions were varied to make the forces on the ions zero and in the case of noncubic structures, e.g., T-12, β-tin, the c/a ratio was varied to make the stress isotropic. Since both the forces and stresses are not variational quantities, more iteration cycles were required to achieve self-consistency in the calculation.

These calculations were performed with *ab initio* nonlocal ionic pseudopotentials,[27] the local-density approximation (LDA) using the Wigner interpolation form for the exchange and correlation energy, and plane-wave basis sets. With these ingredients equilibrium properties of simple crystals (i.e., bulk modulii, elastic constants, phonon frequencies, etc.) have been calculated to be accurate to within a few percent of experiment,[26] and pressure-induced transitions to many simple metallic phases have been described well.[28] A shortcoming however, of the present formalism, particularly of the LDA, are the much smaller energy gaps between the valence and unoccupied states in insulators.

IV. COMPLEX TETRAHEDRAL PHASES OF SILICON

We have used the density-functional calculations to produce results for Si, summarized in Fig. 3, that show the energy of the diamond, β-tin, and fully relaxed B-8 structures as a function of the atomic volume, where $V_0 = 20.024$ Å^3 is the experimental diamond-structure Si volume. Relaxation of the B-8 structure involved calculations of the force F on the ions, for two different internal parameters x (at constant volume), from which the bond-stretching force constant k for the A bonds was extracted. Knowing k, the internal parameter that relaxes the structure at each volume was then determined.

Though the calculations for the large unit cell B-8 are much more difficult than for the simple structures previously considered, we have performed the calculations with comparable accuracy to previous work.[28] The basis set for all Si calculations was plane waves up to 12 Ry in energy, corresponding to ~84 plane waves/atom near $V/V_0 = 0.9$. Plane waves from 6 to 12 Ry were treated with the second-order Löwdin scheme,[29] that includes the perturbative expansion of the wave functions and charge densities in terms of the Löwdin waves. The Löwdin scheme is a tractable way of handling the large Hamiltonian matrices in the complex structures. The basis set
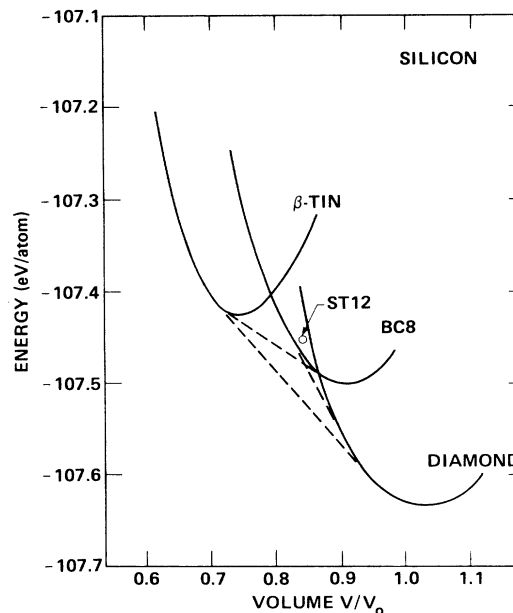
FIG. 3. Energy of silicon in the relaxed B-8, diamond, and β-tin phases as a function of reduced volume. The T-12 energy is shown at one volume. The dashed common tangent lines show that the stable phases under pressure are diamond and β-tin. B-8 and T-12 are at slightly higher enthalpy and may be formed only metastably.

for B-8 comprised of ~225 exact and 450 Löwdin waves near $V/V_0 = 0.9$, illustrating the size of the computations.

For the calculations shown in Fig. 3, integrations over the Brillouin zone were performed with **k** sets of 1, 2, 4, and 7 points for B-8; 2 and 10 points for diamond; and 1 and 6 points for T-12. While the smaller sets were adequate for relative energies within each phase, the absolute energies or energy differences between the phases were fixed with the respective 7-, 10-, and 6-k-point calculations. A large number of points (40) was used for the metallic β-tin.

The curves of Fig. 3 are obtained from fitting the calculated energies at 7, 5 and 8 volumes in the diamond, B-8 and β-tin phases, respectively, to the first-order Murnaghan equation of state[30]

$$E - E_0 = \frac{B_0 V}{B_0'(B_0' - 1)} [B_0'(1 - V_0/V) + (V_0/V)^{B_0'} - 1] ,$$

$$(5)$$

which is derived from the assumption that the bulk modulus B_0 varies linearly with the pressure

$$B(P) = B_0 + B_0' P .$$

$$(6)$$

In the present work, the Murnaghan equation has been mainly used to connect the calculated energies with smooth curves. Energy-volume curves have *not* been extrapolated. Since the first-order Murnaghan equation [based on Eq. (5)] is expected to be valid for pressures $P < B_0$, more consistent values of the bulk modulus and its derivative may be obtained from a second-order Mur-

naghan equation [based on $B(P) = B_0 + B'P + \frac{1}{2}B''P^2$].

The structural properties of B-8 are first described, followed by a discussion of its metastability, and an account of the properties of T-12.

A. Properties of the B-8 phase

From these calculations we find the equilibrium B-8 structure at $V/V_0 = 0.903$ and $x = 0.1022$ in satisfactory agreement with the experimental results, $V/V_0 = 0.912$ and $x = 0.1003 \pm 0.0008$.[6] The calculated equilibrium structure with the parameter $x = 0.1022$, leads to bond angles of $AB = 98.42°$, $BB = 117.89°$, and bond lengths $R_A = 2.341$ Å, $R_B = 2.377$ Å. The minimum energy for B-8 is calculated to be 0.13 eV per atom higher than that of diamond. Fits to the Murnaghan equation of state over the full volume range, provided the quantities $B_0 = 918$ kbar, and $B'_0 \simeq 3.79$, for B-8.

The enthalpy difference between the B-8 and diamond phases decreases with pressure, and the two phases are equally stable at the points given by the common tangent between B-8 and diamond shown in Fig. 3. The relaxation of the B-8 structure causes the internal parameter x to increase to 0.105 at the transition point, i.e., the bond angles are further distorted from tetrahedral ($\sphericalangle AB \simeq 97.41°$; $\sphericalangle BB \simeq 118.36°$) and more remarkably, the difference in the bond lengths $R_A - R_B$ changes sign with pressure ($R_A = 2.329$ Å; $R_B = 2.293$ Å at the transition point)—the structure now having one long (A) bond and three shorter (B) bonds. This prediction of the reversal of the relative bond lengths could be tested by subjecting the experimentally recovered B-8, to pressure again and performing x-ray diffraction measurements.

From the force constant k associated with this internal mode, we estimate that allowing for the structural relaxation lowers the B-8 diamond transition pressure by ~ 15 kbar, i.e., compared to the unrelaxed case with x fixed at the experimental value. Further, the calculation of the force constant k leads to a frequency of 410 cm^{-1} for the Γ_1^+ optic mode which compared well with Raman measurements[31] of 416 ± 2 cm^{-1}. This Raman mode corresponds to a compression of the A bonds and is significantly softer than the 520 cm^{-1} optic mode of diamond silicon. The interpretation of the softening is that covalent bonds are slightly weaker in B-8 than diamond despite the increase in density.

We have examined the electronic structure of B-8 silicon and Fig. 4 shows the energies of the two states around the Fermi level, at various high-symmetry points in the Brillouin zone which are labeled with the usual conventions.[8] The calculation was for a slightly compressed B-8 volume ($V/V_0 = 0.86$ with $x = 0.1037$). Within the limitations of the LDA, these calculations find B-8 Si to be semimetallic, with the valence and conduction bands touching at the H point of the Brillouin zone, in a triply degenerate state. As indicated in Fig. 4, there is band overlap of ~ 0.34 eV between the zone boundary points H and F, leading to a small, semimetallic Fermi surface. An extremely small overlap also exists between H and N. These results are different from previous empirical pseudopotential calculations[8] which found a direct gap at H of
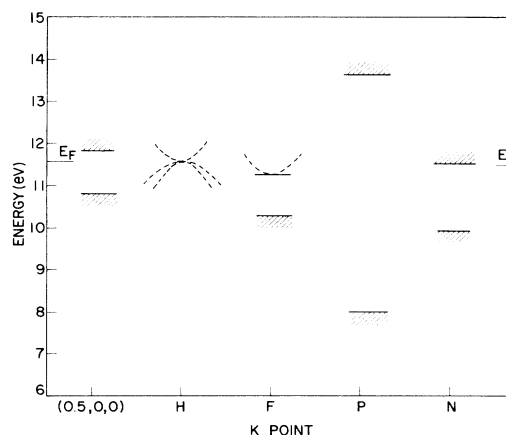
FIG. 4. Schematic plot of the conduction-band minima and valence-band maxima for B-8 Si, at high-symmetry points in the Brillouin zone (using conventions of Ref. 8). B-8 Si is semimetallic at H and the structure of the touching bands is shown. There is an overlap between H and F.

0.43 eV, caused by a different ordering of states at H. However, the band touching feature at H was found in the previous calculations for B-8 germanium.[8] The semimetallic character or the small energy gaps, as well as the presence of many-conduction-band valleys, may be a source of novel electrical properties for B-8. We should note, however, that the semimetallic nature of B-8 calculated here may be a consequence of the well-known deficiency of the local-density approximation of yielding band gaps that are substantially smaller than experiment. We cannot resolve this point here.

We have made a simple estimate of the inaccuracy of our total energies, that result from not accounting for the semimetallic properties of B-8 Si. This estimate is based on the result, derived by Janak,[32] that the variation of the
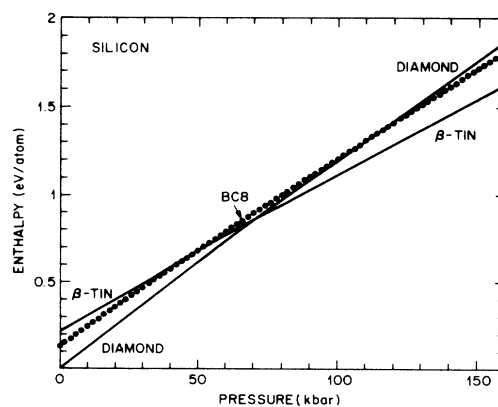
FIG. 5. Enthalpy $H = E + PV$ of diamond, B-8, and β-tin silicon phases as a function of pressure relative to the diamond phase at zero pressure. β-tin is the stable phase above 70 kbar. B-8 is metastable, close in enthalpy to the stable phases.

density-functional total energy E_{tot} with respect to the state occupation f_i, is the variational energy eigenvalue ε_i of that state:

$$\delta E_{tot}/\delta f_i = \varepsilon_i \qquad (7a)$$

Equation (7a) provides an interpretation for the energy eigenvalues of density-functional theory. Small total energy differences from the ground state can then be estimated with the one-electron energies. The energy difference caused by slightly changing the populations of states is then

$$\delta E_{tot} = \sum_i \delta f_i \varepsilon_i \ . \qquad (7b)$$

For B-8 Si, we find, in our calculations, a small Fermi surface that contains at most 0.2 electrons out of a total of 32 electrons/cell, thus causing an energy change of < 0.005 eV/atom. The B-8 total energies are thus insensitive to its semimetallic character.

B. Metastability of B-8 Si

The relative stability of the different structures has been examined by performing calculations on diamond and β-tin with the same plane-wave cutoffs as for B-8, leading to the results illustrated in Figs. 3 and 5. For the β-tin energy curve of Fig 3, the c/a ratio was varied to make the two inequivalent components of the stress equal. As is evident from Fig. 3 there is a first-order transition from the diamond to β-tin structures at a pressure, given by the common tangent between the two phases, which we calculate to be ~ 70 kbar. These calculations provide transition volumes that compare very well (within 2 percent) to those of Yin and Cohen,[28] though a somewhat lower transition pressure.

The relative stability of the structures is more clearly evident from Figs. 5 which plots the enthalpy of diamond, β-tin, and B-8 as a function of pressure. Although B-8 becomes more stable than diamond above 107 kbar, the lowest enthalpy states or stable phases are diamond at low pressures and β-tin at pressures above 70 kbar. The β-tin phase transforms further to the simple hexagonal phase at a calculated pressure of ~ 80 kbar.[33] B-8 has an enthalpy only slightly higher than these phases at all pressures. This implies that B-8 may only be formed as a metastable phase over all pressure ranges for silicon, which is consistent with the experimental findings.[5,7] Further, the B-8 enthalpy is in between that of diamond and β-tin at pressures below ~ 45 kbar and above ~ 107 kbar. Figure 5 indicates that if the β-tin to diamond transition is inhibited by kinetic considerations at the metallization pressure (~ 70 kbar in Fig. 5), β-tin may in fact transform to B-8 at the lower pressure of ~ 45 kbar where B-8 is more stable than β-tin.

The metastability of B-8 relative to diamond at ambient pressures can be understood by examining a shear distortion path between the B-8 and diamond structures. This shear path involves a sliding of double layers of diamond. Since diamond and B-8 are topologically very different, this transformation requires breaking and reforming as many as one-quarter of all tetrahedral bonds. This large bond-breaking implies a high-energy barrier between diamond and B-8, and indicates why B-8 can remain metastable relative to diamond at zero pressure.

It is worth noting that similar transition paths can be constructed between B-8 and wurtzite. Fewer bonds are broken in this transformation, than between B-8 and diamond. This suggests why B-8 is often converted to wurtzite silicon on thermal annealing.

The phase transformation from the metallic β-tin phase to B-8 or diamond involves complex kinetic considerations. The added metallic coordination of β-tin makes it easier to transform between metallic β-tin and insulating structures, than between two insulating structures that are topologically dissimilar, and only very-high-symmetry distortion paths between β-tin and diamond have been investigated.[34]

In experiments, the Si samples break up into a polycrystalline form on transition to the β-tin phase. This microcrystalline nature of β-tin along with the presence of grain boundaries and defects, may ease the nucleation of complex phases like B-8 and T-12, from β-tin. The kinetics of phase transformations may be an aspect for further studies, particularly with molecular-dynamics simulations using classical interatomic Si potentials.

Our calculation of 70 kbar for the diamond β-tin transition pressure needs to be scaled upwards to compare with the experimental value of ~ 125 kbar. This scaling may represent inherent inaccuracies of the density-functional calculation. The calculated pressure of 107 kbar for the point at which diamond and B-8 are equally stable, could also scale upwards in the same way, implying that B-8 is metastable. However an alternative possibility is that the corrections for B-8 and diamond are very similar since they have similar local bonding, but quite different for metallic β-tin. If the value of 107 kbar compares well with experiment, this would imply that B-8 Si is a stable phase over a narrow range of pressures (107 kbar to 125 kbar).

C. T-12

In comparison to B-8, T-12 has five structural degrees of freedom and, lacks a center of inversion, resulting in a complex Hamiltonian matrix that makes calculations for T-12 much more difficult than for B-8. A calculation at one volume for T-12 is indicated in Fig. 3. For this calculation the five free parameters of T-12 were approximately relaxed. The important result is that the T-12 structure was close in energy to B-8, both structures then being almost stable in silicon. The energy differences between these structures and diamond, are close to that measured (0.123±.007 eV/atom) for amorphous silicon,[35] through calorimetry experiments, suggesting there may be a number of topologically different structures with locally similar distorted tetrahedral bonding that have similar energies. This is also supported by calculations of distorted tetrahedral structures with 16 to 20 atoms/cell.[36] These were found to be only slightly higher energy than diamond (~ 0.01 eV/atom).[36] Generally the local tetrahedral distortions of these phases are smaller than in B-8 and T-12, but lead to larger unit cells.

The relaxation of the T-12 structure was achieved with calculations of the forces and stresses (F_i), which were used to construct a force matrix C_{ij} through

$$E - E_0 = \tfrac{1}{2} \sum_{ij} X_i C_{ij} X_j \tag{8}$$

and

$$F_i = \partial E / \partial X_i = \sum_j C_{ij} X_j . \tag{9}$$

Here the definition of F_j is generalized to include the stresses and X_i is the structural parameter conjugate to F_i. For T-12, the X_i were chosen to be $(V - V_{eq})/V_{eq}$, $e_3 - \tfrac{1}{3}(e_1 + e_2 + e_3)$, α, x, y, and z, resulting in the quantities F_i being PV_{eq}, $(\sigma_{zz} - \sigma_{xx})$ and the fa, where f were the appropriate conjugate forces in the unit cell and a the lattice constant. V_{eq} is the true equilibrium T-12 volume, e_i's are the elastic strains and σ_{xx}, σ_{zz} the stresses.

Calculations of the forces F_i's were performed on changing each X_i separately, and led to the construction of the full 6×6 C_{ij} matrix through

$$\frac{\partial F_i}{\partial X_k} = C_{ik} , \tag{10}$$

and six pairs of calculations. However the matrix C_{ij} was found to be asymmetric due to the numerical noise involved in computing small differences between forces that themselves were small. A further attempt to determine the equilibrium structure seemed unwarranted. The different partially relaxed configurations resulting from changing each X_i separately, differed in total energy by ≤ 0.017 eV/atom at the volume shown in Fig. 3.

Perhaps ab initio methods that use localized basis sets[37] may be less susceptible to such numerical problems and may be useful for future work on such complex systems. T-12 may be ideally suited for studies with recently developed molecular-dynamics simulated annealing techniques within the LDA,[38] or with accurate classical two- and three-body interatomic potential models of silicon.[39] In fact, the structural energies of insulating and metallic structures, such as presented here has been the key input in developing such accurate classical potentials that globally model energies of Si structures.

These calculations revealed a remarkable soft mode of T-12. This mode involves a rotation of the two spirals of the unit cell, in opposite senses relative to each other, and a relative displacement of the spirals along the z axis. Thus, each spiral undergoes a screw motion in opposite senses. This mode is associated with bond-bending forces only between the A,C; A,B; and B,C bonds, which accounts for its low energy, and should give rise to a low-frequency Γ_1 phonon. In comparison, bond-stretching forces are large and displacements that distort the shape of the spirals are energetically expensive. The energy calculations for T-12 indicate that its bulk modulus may not be as low as previously predicted.[40]

Useful information on the electronic structure was obtained from the 6-k-point calculations. We found the top of the valence band to vary between 10.02 and 10.62 eV, and the bottom of the conduction band between 12.19 and 12.76 eV, with direct gaps ranging between 1.73 and 2.40

eV and a smallest indirect gap of 1.57 eV. These calculations then suggest relatively flat valence and conduction bands in T-12, in agreement with the empirical pseudopotential calculations of Ref. 8. The energy gaps of T-12 are generally larger than those calculated for diamond-Si with this LDA method. It has been argued quite generally[8] that the presence of odd-membered rings removes states away from the gap, whereas the presence of distorted even-membered rings introduces states into the gap, and this feature is supported by the present B-8 and T-12 calculations. A well-defined gap in the densities of electronic states is also present in amorphous silicon.

V. THE STABILITY OF CARBON

The discussion of silicon leads to interesting consequences for the high-pressure phase diagram of carbon. The stability of diamond-carbon is important in setting an upper limit to pressures that may be achieved in diamond anvil cells. Previous calculations by Yin and Cohen[17] found that the simple metallic phases (e.g., fcc, bcc, β-tin) were much higher in energy than diamond, and had equilibrium volumes very close to, or even larger than diamond. This led to the prediction that diamond was more stable than all the simple metallic phases considered up to a pressure of 23 Mbar (where the volume is compressed to $\tfrac{1}{3} V_0$), at which point the simple cubic phase becomes more stable.

However, on the basis of simple tetrahedral packing considerations, the complex phases (B-8 and T-12) would be expected to have equilibrium volumes smaller than the diamond, and further, should be lower in energy than the metallic phases. This suggests that these complex structures can be stable phases of carbon under pressure, and more stable than diamond at a large enough pressure. We have investigated the stability of carbon in diamond, B-8, and the structure proposed in Ref. 41.

To establish the accuracy of our calculations for carbon, we first show the calculations of energy versus volume for diamond in Fig. 6. These calculations were performed with constant basis sets which produces smoother energy-volume curves (and hence more consistent values of the calculated pressures), than the method of constant energy cutoffs (which was used for silicon). Many more plane waves are required for convergence for carbon, than for silicon, since the absence of p electrons in the carbon core allows the valence p electrons to approach closer to the carbon nucleus. Consequently a very large basis set of 215 exact plane waves/atom was used for diamond (corresponding to an energy cutoff of 50 Ry near equilibrium and ~ 80 Ry near the transition), and the resulting energy-volume curve is shown as diamond A in Fig. 6. Fitting this curve over the full volume range to the Murnaghan equation of state led to the equilibrium properties of $V/V_0 = 0.982$, $B = 4.94$ Mbar, $dB/dP = 2.6$, in good agreement with previous calculations[17,37] and experiment[21] ($V_0 = 5.673$ Å^3, $B = 4.42$ Mbar, $dB/dP \sim 4$).

However a comparison of B-8 and diamond necessitates calculations of similar accuracy in the two structures and for this purpose a smaller basis set of ~ 85 plane

waves/atom (approximately half were treated by Löwdin perturbation theory) was used for the diamond B curve in Fig. 6. Comparison of the curves A and B shows the important result that, although the larger basis set is needed near the equilibrium volumes, the smaller basis set becomes increasingly sufficient (and the calculations B increasingly accurate) at the reduced volumes near the predicted transition.

The reason the diamond A and B curves approach each other closely at the small volumes is related to the kinetic piece of the total energy increasing very rapidly ($\sim 1/r_s^2$) under compression. At the compressed volume, the potential in the Hamiltonian matrix appears much weaker relative to the kinetic part, and the basis set becomes more complete. It is worth noting that the energy difference between A and B is a simple function of the volume ($\delta E \sim V^{4.5}$).

Consequently the diamond B curve is compared with a calculation of the B-8 carbon energy at compressed volumes in Fig. 7. Both diamond B and B-8 curves have the same basis set (~ 85 plane waves/atom). The inset shows that B-8 is lower in energy than diamond for $V/V_0 < 0.45$ and well below the simple cubic phase taken from Ref. 17. B-8 becomes more stable than diamond at a pressure of 12 Mbar—the slope of the common tangent between B-8 and diamond. The transition between these two phases involves a small volume change of $\approx 0.011V_0$.

The transition can alternatively be seen from Fig. 8

which is a plot of the enthalpy $H = E + PV$, as a function of the pressure. The solid lines are from the fitted equations of state of energy versus volume, whereas the points are from direct calculations of energy and pressure. That the points are on the fitted curves demonstrates the consistency of computing pressures, and also that from a few calculations of the pressure and energy, one can infer the transition and estimate the transition pressure to within 10%.

In performing the B-8 calculations, the B-8 structure was relaxed as in the Si calculations. The calculated internal parameter varied from 0.0955 at $V/V_0 = 0.85$ to 0.1030 at $V/V_0 = 0.45$, implying a change of bond angles of $< 1°$ over this large volume range illustrative of the large bond-bending forces in carbon. As in Si the conduction bands touch at H so that there is no gap within the LDA, though large direct gaps were present at other tested points in the zone.

Also shown in Fig. 7 is a calculation for a proposed distorted tetrahedral structure[41] of Matyushenko, Stiel'nitskii, and Gusev (MSG) that consists of 8-atom cubes arranged on a bcc lattice, producing bond angles of 90° and 125°. Although this structure is also body-centered cubic with 8 atoms per cell, it has the full symmetry of the cubic group. We find that this MSG structure has both higher energy and higher pressure than B-8,

FIG. 6. Energy of carbon in the diamond phase as a function of reduced volume. Curves A and B are for larger and smaller basis sets and show that the smaller set used for B and for B-8 are accurate at small volumes near the transition.
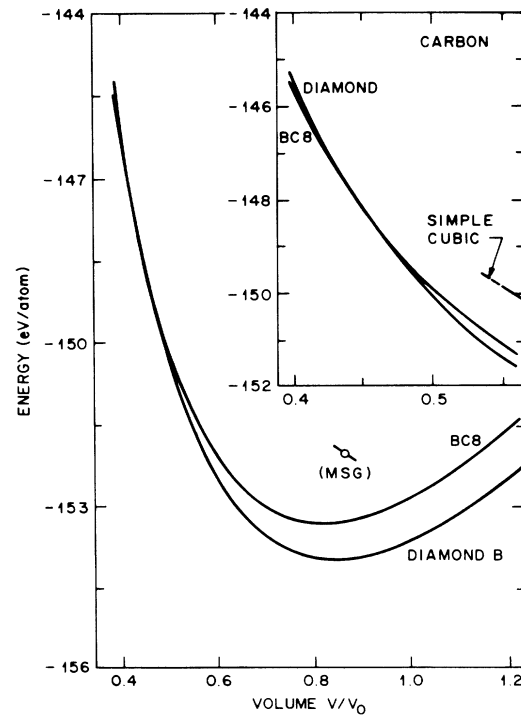
FIG. 7. Energy of carbon in the diamond and B-8 phases. Calculations use the smaller basis set. The inset is an expanded view of the region where B-8 becomes more stable than diamond. The energy of simple cubic from Ref. 17 is shown for comparison. The 8 atoms/unit cell structure proposed in Ref. 41 is both higher in energy and pressure.
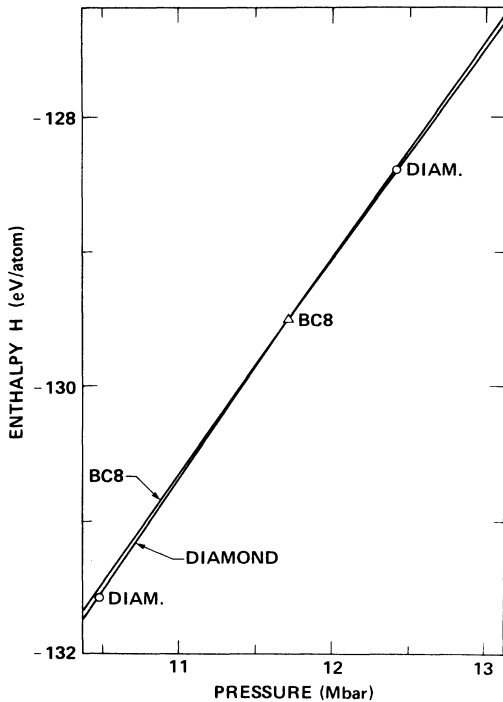
FIG. 8. Enthalpy $H = E + PV$ of carbon in the diamond and B-8 phases as a function of pressure P, showing the transition at 12 Mbar. The points are calculated directly and the curves are fitted equations of state from Fig. 7.

indicating that it is not likely to be either a stable or metastable structure. However, it is possible that in the Soviet experiment (MSG) the B-8 carbon structure was instead synthesized, since both the MSG and B-8 structures have very similar diffraction patterns and the measured volume was very close to that expected for equilibrium B-8.

To ascertain the sensitivity of these results to the pseudopotential used,[42] we examined the different and more accurate pseudopotential[43] which has a smaller core radius and consequently required many more plane waves for convergence. A calculation with as many as ~ 400 plane waves/atom for diamond at $V/V_0 = 0.48$, yielded pressures very similar to those previously computed, suggesting that the details of the potential are unimportant for these conclusions.

A qualification on these results concerns the phonon energies, which have not been included in the ground-state total energies shown for silicon and carbon. The Debye temperatures (energies) of Si and C are 625 K (0.062 eV/atom) and 1860 K (0.185 eV/atom), respectively, and the zero-point energies can be simply estimated as $\frac{9}{8}$ of the Debye energies. Though the zero-point energies appear large on the scale of Fig. 3, it is the differences in the vibrational energies between the different structures that would alter the relative energies of the phases. The magnitude of such vibrational energy differences is difficult to estimate with the present calculations, since it requires computations of low-symmetry phonon energies in the large unit-cell structures. However, calculations of the

phonon spectrum in B-8 and diamond-structure silicon have been performed,[44] using the adiabatic bond charge model. The calculated densities of one-phonon states appears similar in the B-8 and diamond structures[44] suggesting that the vibrational energy differences between the two phases may be small.

Generally the distorted tetrahedral structures have weaker bonds and may be expected to have softer phonons (and larger vibrational energies) than diamond, leading to an increase in the B-8 diamond energy difference. An estimate of the contributions of the vibrational energies to the relative stability of these structures may be an aspect for further study.

VI. CONCLUSIONS

In summary, we have examined the structural stability of Si and C in the complex tetrahedral and diamond structures (and for Si, β-tin also), with ab initio calculations of total energies, forces, and stresses. We find the complex tetrahedral B-8 Si structure to have enthalpy only slightly higher than the stable phases (diamond at low pressures and β-tin at higher pressures). This is consistent with the experimental finding of the metastability of B-8 and T-12 Si, and their formation during pressure reduction in high-pressure experiments. B-8 Si is slightly semimetallic, whereas T-12 Si has an indirect gap larger than diamond-structure Si. A zone-center optic vibration frequency for B-8 Si has been computed, and agrees well with experiment. The determined zero-pressure structural geometry from the present calculations also agrees well with x-ray diffraction determinations of the complex structures. New predictions are made for a reversal of the bond lengths of B-8 Si under pressure and for an unusual soft mode of T-12.

For carbon we have found a new stability limit of diamond of 12 Mbar, at which point it becomes more favorable for the tetrahedra to distort and pack more closely in the B-8 phase. Although this is a high pressure, it is much lower than the pressure of 23 Mbar found previously[16] for transitions to simple metallic phases. However, it is always possible that diamond may transform to another structure, not considered so far, at a pressure lower than 12 Mbar. Also uniaxial stresses may lead to transitions at lower pressures[45] than 12 Mbar found here. These conclusions on the stability of diamond rest upon the assumptions of the LDA and rigid ionic pseudopotentials at the greatly compressed volumes. The latter could be checked by all electron calculations.

[1]J. C. Jamieson, Science **139**, 762 (1963).

[2]B. Weinstein and G. J. Piermanni, Phys. Rev. B **12**, 1172 (1975).

[3]H. Olijnk, S. K. Sikka, and W. B. Holzapel, Phys. Lett. **103A**, 137 (1984).

[4]K. J. Chang, N. M. Dacorogna, M. L. Cohen, J. M. Mignot, G. Chouteau, and G. Martinez, Phys. Rev. Lett. **54**, 2375 (1985).

[5]Y. K. Vohra, K. E. Brister, S. Desgreniers, A. L. Ruoff, K. J. Chang, and M. L. Cohen, Phys. Rev. Lett. **56**, 1944 (1986).

[6]R. H. Wentorf, Jr. and J. S. Kaspar, Science **139**, 338 (1963); J. S. Kaspar and S. M. Richards, Acta. Cryst. **17**, 752 (1964).

[7]F. P. Bundy and J. S. Kaspar, Science **139**, 340 (1963).

[8]J. D. Joannopoulos and M. L. Cohen in, *Solid State Physics* (Academic, New York, 1976), Vol. 31, p. 71; Phys. Rev. B **7**, 2644 (1973).

[9]M. D. Vaugin, B. Cunningham, and D. G. Ast, Scr. Metallurgica **17**, 191 (1983), and references therein.

[10]D. P. DiVincenzo, O. L. Alerhand, M. Schluter,, and J. W. Wilkins, Phys. Rev. Lett. **56**, 1925 (1986).

[11]K. C. Pandey, Phys. Rev. Lett. **47**, 1913 (1981).

[12]F. P. Bundy, J. Geophys. Res. **85**, 6930 (1980); J. E. Field, *The Properties of Diamond* (Academic, London, 1979).

[13]H. K. Mao and P. M. Bell, Science **200**, 1145 (1978).

[14]See, e.g., A. E. Carlsson and N. W. Ashcroft, Phys. Rev. Lett. **50**, 1305 (1983).

[15]See, for example, the review by A. Jayaraman, Rev. Mod. Phys. **55**, 65 (1983).

[16]J. A. Van Vechten, Phys. Status Solidi B **47**, 261 (1971).

[17]M. T. Yin and M. L. Cohen, Phys. Rev. Lett. **50**, 2006 (1983).

[18]R. Biswas, R. M. Martin, R. J. Needs, and O. H. Nielsen, Phys. Rev. B **30**, 3210 (1984).

[19]M. T. Yin, Phys. Rev. B **30**, 1773 (1984).

[20]*International Tables for X-Ray Crystallography* (Riedel, Dordrect, Holland, 1983), Vol. A.

[21]J. Donohue, *The Structures of the Elements* (Wiley, New York, 1974).

[22]See, for example, D. J. Chadi, Phys. Rev. Lett. **43**, 43 (1979).

[23]P. Hohenberg and W. Kohn, Phys. Rev. **136**, B864 (1964); W. Kohn and L. J. Sham, *ibid.* **140**, A1133 (1965).

[24]R. M. Martin and K. Kunc, in *Ab initio Calculations of Phonon Spectra* (Plenum, New York, 1983).

[25]J. Ihm, A. Zinger, and M. L. Cohen, J. Phys. C **12**, 4409 (1979).

[26]O. H. Nielsen and R. M. Martin, Phys. Rev. Lett. **28**, 697 (1983).

[27]D. R. Hamann, M. Schluter, and C. Chiang, Phys. Rev. Lett. **43**, 1494 (1979).

[28]M. T. Yin and M. L. Cohen, Phys. Rev. B **26**, 5668 (1982).

[29]P. O. Löwdin, J. Chem. Phys. **19**, 1396 (1951).

[30]F. D. Murnaghan, Proc. Natl. Acad. Sci. **30**, 214 (1944).

[31]R. J. Kobliska, S. A. Solin, M. Selders, R. K. Chang, R. Alben, M. F. Thorpe, and D. Weaire, Phys. Rev. Lett. **29**, 725 (1972).

[32]J. F. Janak, Phys. Rev. B **18**, 7165 (1978).

[33]R. J. Needs and R. M. Martin, Phys. Rev. B **30**, 5372 (1984).

[34]R. Biswas and M. Kertesz, Phys. Rev. B **29**, 1791 (1984).

[35]J. M. Poate, Nucl. Instrum. Methods **209**, 211 (1983).

[36]D. J. Chadi, Phys. Rev. B **32**, 6485 (1985).

[37]J. R. Chelikowsky and S. G. Louie, Phys. Rev. B **29**, 3470 (1984).

[38]R. Car and M. Parrinello, Phys. Rev. Lett. **55**, 2471 (1985).

[39]R. Biswas and D. R. Hamann, Phys. Rev. Lett. **55**, 2001 (1985).

[40]R. Alben and D. Weaire, Phys. Rev. B **9**, 1975 (1974).

[41]N. N. Matyushenko, V. E. Strel'nitskii, and V. A. Gusev, Pis'ma Zh. Eksp. Teor. Fiz. **30**, 218 (1979). [JETP Lett. **30**, 199 (1979)]. The proposed structure had 8-atom cubes placed on a bcc lattice with bond angles of 90° and 125°.

[42]G. B. Bachelet, H. S. Greenside, G. A. Baraff, and M. Schluter, Phys. Rev. B **24**, 4745 (1981).

[43]G. B. Bachelet, D. R. Hamann, and M. Schlüter, Phys. Rev. B **26**, 4199 (1982).

[44]A. Goldberg, M. El-Batanouny, and F. Wooten, Phys. Rev. B **26**, 6661 (1982).

[45]O. H. Nielsen, Phys. Rev. B **34**, 5808 (1986).